THERMAL ACOUSTIC SENSOR FOR HIGH PULSE ENERGY X-RAY FEL BEAMS*

T.J. Smith#, J.C. Frisch, , E.M. Kraft, J. Loos, SLAC, Menlo Park, CA 94025, U.S.A.
G.S. Bentsen, University of Rochester, Rochester, NY 14627, U.S.A.

Abstract

The pulse energy density of X-ray FELs will saturate or destroy conventional X-ray diagnostics, and the use of large beam attenuation will result in a beam that is dominated by harmonics. We present preliminary results at the LCLS from a pulse energy detector based on the thermal acoustic effect. In this type of detector an X-ray resistant material (boron carbide in this system) intercepts the beam. The pulse heating of the target material produces an acoustic pulse that can be detected with high frequency microphones to produce a signal that is linear in the absorbed energy.

INTRODUCTION

The thermal acoustic detector is designed to provide first- and second-order calorimetric measurement of X-ray FEL pulse energy. The first-order calorimetry is a direct temperature measurement of a target designed to absorb all or most of the FEL pulse power with minimal heat leak. The second-order measurement detects the vibration caused by the rapid thermoelastic expansion of the target material each time it absorbs a photon pulse. Both the temperature change and the amplitude of the acoustic signal are directly related to the photon pulse energy.

DESIGN

The Detector

The thermal acoustic detector (Fig. 1) consists of a target block of boron carbide (B_4C) 12.5 x 10.0 x 8.0 mm (w x h x L) mechanically secured between a set screw and two piezoelectric detectors. The target thickness allows complete absorption of FEL energies < ~7 keV, with some roll-off in the hard x-ray regime (~7% transmission at 10 keV). Two 500 Ω thin film platinum resistive temperature detectors (RTDs) are affixed to the opposite faces. The target sits 5 mm downstream of a gun barrel collimator, a Tungsten block with a 5 mm hole aligned to the center of the B_4C target, to shield the target from higher harmonics of the FEL and spontaneous halo. The collimator is shielded by a B_4C mask to protect the high-Z tungsten from low energy X-rays.

The target and shield assembly is affixed to a large solid aluminum base which provides a thermal mass sufficient to maintain the tungsten shield, the set screw and the rest of the assembly at an approximately constant temperature over the course of a measurement. Single-strand AWG-32 copper signal wires pass from the acoustic sensors and the RTD leads to a UHV-compatible breakout PCB on the downstream side of the aluminum support base. An additional reference RTD is affixed to the aluminum base to monitor ambient temperature variation. The sensor signals are brought from within the UHV chamber to a local instrumentation crate where the sensor signals are filtered and amplified and the RTD signals are converted to temperature readings. The local crate also provides the option to drive either RTD as a resistive heat source to calibrate the thermal system. A YAG profile monitor downstream is used to verify alignment of the target with the x-ray beam.

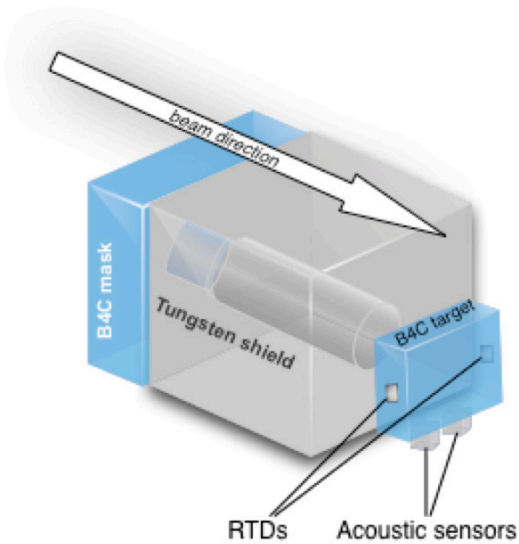

Figure 1: Configuration of the target, shielding and detectors.

Thermal

The temperature of the target block is monitored by two 500 Ω platinum RTDs (US Sensor PPG501A1), bonded to either side of the block with Hysol 1C UHV-compatible epoxy (Torr-Seal). A reference RTD is bonded to the massive aluminum base on which the detector rests to monitor fluctuations in ambient temperature. Each RTD lead is broken out to two wires for 4-wire ratiometric resistance measurements. Heat exchange between the target and surroundings is primarily (~60%) from conduction through the piezoelectric elements, but radiation is also significant.

Acoustic

The piezoelectric detectors (Physik Instrumente PICMA PL-033) are 3 x 3 x 2 mm monolithic multilayer actuators with 22 nm/V unloaded displacement and > 300

*Work supported by Department of Energy Contract DE AC03 76SF00515
#tonee@slac.stanford.edu

ISBN 978-3-95450-117-5

kHz resonant frequency. The parallel configuration of the piezoelectric elements in this model is optimized for translating a small signal into a large displacement, instead of turning a small displacement into a large signal as desired in a detector. Nevertheless, this component was chosen for its compact form factor, UHV compatibility, and orthogonal orientation of the electrodes to the axis of displacement.

The frequency of the detector was chosen such that $\omega_d \sim s/D$, where s is the acoustic wave velocity (in B_4C = 10920 m/s), and $D = 2 * L$, where L is the target block dimension normal to the acoustic sensors (10 mm) [1]. The predicted resonance of our system is ~545 kHz. The measured resonance peaks at 531 kHz.

Preliminary Results

First data sets were collected at photon energies of 5 keV and 8.3 keV. Digitized acoustic sensor waveforms (Fig. 2) and RTD data were logged at 1 Hz under lasing, suppressed, and beam-off conditions.

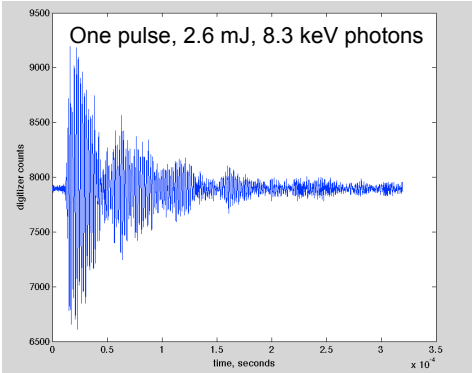

Figure 2: Acoustic response from a single 2.6 mJ pulse of 8.3 keV x-rays, 25 MHz digitizer clock.

The waveforms were processed to extract the amplitude of the resonant peak, with beam-off background spectrum subtracted.

RTD Calibration

Temperature calibration was performed by driving one RTD at a fixed voltage and monitoring the temperature rise on the other until it begins to roll off (Fig. 3).

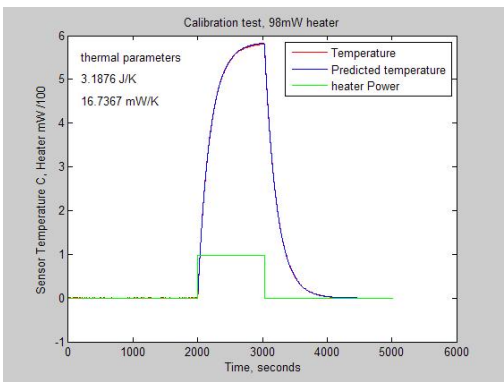

Figure 3: RTD predicted (from empirical fit) and measured response curves.

We empirically optimize an exponential fit to the temperature curve of the monitoring RTD to get coefficients for the thermal mass, the thermal leak and any offset term for the system. Verification of the calibration result is shown by calculating the input driving power from the measured temperature curve (Fig. 4).

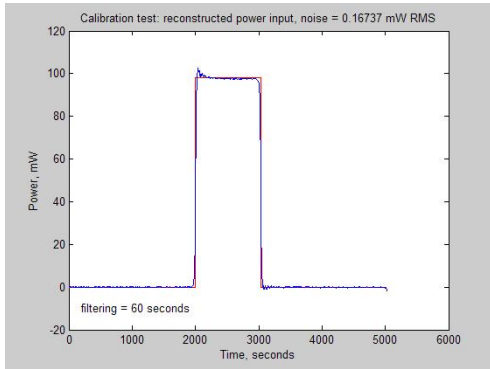

Figure 4: RTD drive power (98 mW) as calculated from temperature response.

The long term stability of the thermal calibration is shown to be better than 200 uW over a four day period with no beam (Fig. 5). This low drift indicates frequent calibration will not be required.

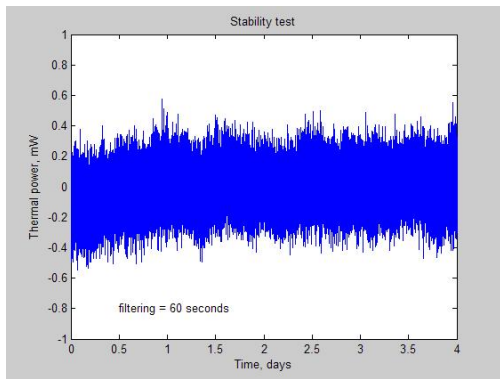

Figure 5: Power calculated from target temperature over four days.

Calibration with Beam

With the RTDs calibrated to measure energy absorbed by the target, we compare the target temperature changes to the response of the acoustic detectors. Data acquisition is 1 Hz, FEL is 120Hz.

For 5 keV photons (Fig. 6), the calibrated acoustic sensor (AS) response agrees well with the canonical energy-loss scan results (calibration factor = 54.2 counts/mJ). Pulse to pulse variation in the AS signal is consistent with the FEL intensity noise as seen on the FEE (Far End Enclosure, the LCLS FEL diagnostics section) gas detectors.

ISBN 978-3-95450-117-5

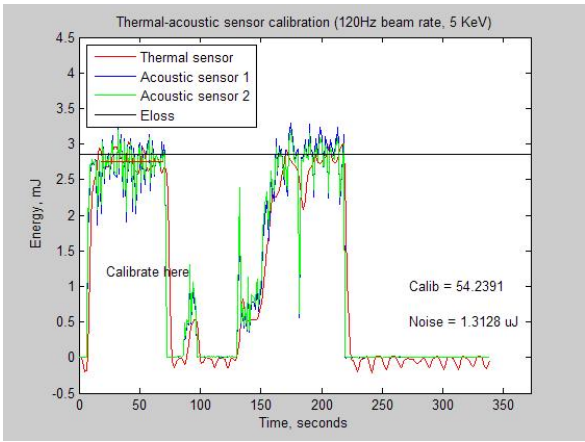

Figure 6: Acoustic and RTD response to 2.86 mJ FEL, spontaneous light (lasing suppressed) and no light.

Data taken at 8.3 keV (Fig. 7) shows a 25% change in the RTD-to-AS calibration coefficient (to 39.4 counts/mJ) beyond the ~1% expected from the decrease in target photon absorption [2], indicating possible nonlinearity at higher energy.

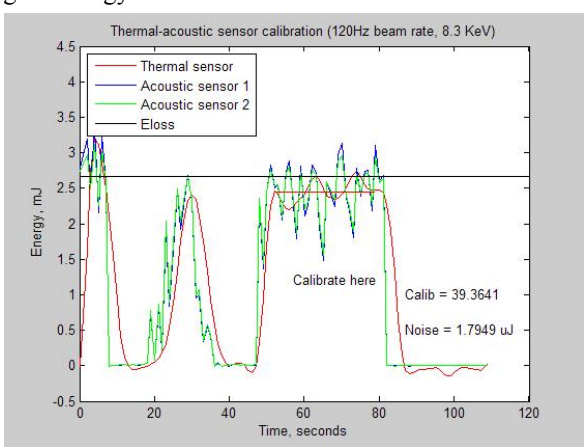

Figure 7: Acoustic and RTD response to 2.67 mJ FEL, including an e-loss scan.

Comparison of the thermal sensor with the energy loss measurement (deriving the FEL pulse energy from the energy lost by the electron bunch under lasing conditions) shows ~10% absolute calibration difference. This is in agreement with the expected accuracy of the energy-loss measurement.

Initial results comparing the two acoustic sensors show some nonlinearity with respect to each other. The effect is similar at both 5 keV and 8.3 keV, suggesting a systematic issue with the sensor electronics, not a radiation acoustics phenomenon. This issue needs further investigation.

Proceeding

Initial results from the thermal acoustic sensor are sufficient to provide proof of principle for the design. Design efforts toward a production model for use in the LCLS experiment hutches is underway.

FUTURE PLANS

- Improve signal processing algorithm, consider broader frequency response.
- Take calibration data at multiple photon energies with longer runs to characterize and correct for thermal time constant of the system.
- Install an active feedback loop on one of the RTDs to hold the target at a fixed temperature. A change in the command drive to the heater as a result of FEL heating of the target provides a direct thermal measurement of pulse power.
- Improve the mechanical design with thermally decoupled collimation.
- Install sensors at experimental stations to monitor transmission losses through the x-ray mirror systems.

CONCLUSIONS

The thermal sensor provides an absolute calibration of beam power with microwatt sensitivity. Preliminary comparison to results from an electron energy-loss scan verifies the accuracy of the E-loss measurement to 10%.

The acoustic sensor provides single shot pulse energy data with < 2 uJ noise and can be calibrated against the thermal sensor.

The target material (B_4C) is compatible with a wide range of photon energies and is suitable for use in high pulse energy FELs.

REFERENCES

[1] A.I. Kalinichenko, V.T. Lazurik, and I.I. Zalyubovsky. *Introduction to Radiation Acoustics*, volume 9 of *The Physics and Technology of Particle and Photon Beams*. Harwood Academic Publishers, 2001.

[2] B.L. Henke, E.M. Gullikson, and J.C. Davis., http://henke.lbl.gov/optical_constants/

ISBN 978-3-95450-117-5